Fluoride Binding in Hemoproteins: The Importance of the Distal Cavity Structure†

Francesca Neri,‡ Donne Kok,‡ Mark A. Miller,§ and Giulietta Smulevich*,‡

Dipartimento di Chimica, Universita' di Firenze, Via G. Capponi 9, 50121 Firenze, Italy, and Department of Chemistry, University of California at San Diego, La Jolla, California 92093

Received February 3, 1997; Revised Manuscript Received May 1, 1997⊗

ABSTRACT: The electronic absorption and resonance Raman spectra of the fluoride complexes of various peroxidases and selected site-directed mutants have been studied at pH 5.0, and compared to the spectra obtained for the myoglobin-F adduct. It is shown that the electronic absorption maxima depend on the degree of conjugation between the porphyrin macrocycle and the vinyl substituents. Moreover, it is confirmed that the wavelength of the CT1 band is a sensitive probe of axial ligand polarity and of its interaction with the distal protein residues. The results highlight the different mechanism of stabilization of the fluoride ligand exerted by the distal residues in myoglobin and peroxidases. In peroxidases, the Arg is determinant in controlling the ligand binding via a strong hydrogen bond between the positively charged guanidinium group and the anion. Mutation of Arg to Leu decreases the stability of the complex by 900-fold, suggesting that this interaction stabilizes the complex by 4 kcal/mol. The distal His also contributes to the stability of the fluoride complex, presumably by accepting a proton from HF and hydrogen-bonding, through a water molecule, to the anion. Mutation of His to Leu decreases the stability of the fluoride complex by 30-fold, suggesting that this interaction is much weaker than the interaction with the distal Arg. For Mb, the distal His is solely responsible for stabilization of the exogenous ligand.

It is well-known that heme pocket proximal and distal amino acid residues control ligand binding in hemoproteins. For example, the distal E7 histidine (His64), which is highly conserved in vertebrate globins (Antonini & Brunori, 1971), has been shown to be important in fine-tuning ligand affinities via hydrogen bond stabilization involving the N_ϵ proton [Aime et al. (1996) and references cited therein]. Peroxidases are characterized by an increased polarity of the distal cavity as compared with globins. In fact, in addition to the distal His, an arginine residue is found to be conserved in the peroxidase cavity (Welinder, 1992) which promotes heterolysis of hydrogen peroxide during the catalytic cycle (Poulos & Kraut, 1980; Vitello et al., 1993; Sitter et al., 1985). Furthermore, it has been proposed that the hydrogen bond between the N_δ proton of the distal His and a conserved Asn residue, and/or the presence of the positively charged guanidinium group in the proximity of the distal His, which depresses its pK_a to values between 4 and 5 (Smulevich et al., 1991b), forces the N_ϵ of the imidazole ring to act as a hydrogen bond acceptor. Therefore, the postulated mechanism of hydrogen peroxide decomposition relies on the concerted role played by the distal Arg and His through direct hydrogen bonds and charge stabilization. In particular, it was suggested (Miller et al., 1994) that in the first step of the reaction the peroxide binds to the iron atom and a proton is transferred from the α-oxygen to the distal His to generate the activated complex. The histidine residue then donates the proton to the β-oxygen, a water molecule is dispelled from the heme pocket, and the distal Arg moves toward the iron and hydrogen-bonds to the oxene group leading to compound I. The fact that met-myoglobin (metMb)[1] reacts with H_2O_2 much more slowly than peroxidases (Yonetani & Schleyer, 1967; Allentoff et al., 1992) suggests that a more polar cavity than that present in metMb is required for heterolytic cleavage of the peroxo group (Dawson, 1988). It is of interest, therefore, to understand whether the different cavity characteristics of the globins and peroxidases are also reflected in the binding of other exogenous ligands. Crystal structures of the complexes formed between cytochrome *c* peroxidase (CCP) and CN^-, NO, CO, and F^- revealed that significant changes are induced in the distal cavity upon adduct formation. The distal Arg and His residues are significantly perturbed, and there is a rearrangement of the water molecules present in the active site (Edwards & Poulos, 1990). For the CCP−CN complex, all three distal residues, Arg48, Trp51, and His52, can potentially form hydrogen bonds with the N atom of cyanide; in CCP−F, the ligand is directly hydrogen-bonded to the Trp51 and Arg48 residues, whereas the distal His appears hydrogen-bonded to a water molecule which is in turn strongly interacting with the fluoride. The interaction between Arg48 and F^- is possible because the distal Arg undergoes a conformational change that places it within hydrogen-bonding distance of the F^-

† This work was supported by the Italian Consiglio Nazionale delle Ricerche (CNR) and the Ministero della Ricerca e della Universita' (MURST) (to G.S.).

* Author to whom correspondence should be addressed. E-mail: SMULEV@CHIM.UNIFI.IT.

‡ Universitá di Firenze.

§ University of California at San Diego.

⊗ Abstract published in *Advance ACS Abstracts,* June 15, 1997.

[1] Abbreviations: ARP, *Arthromyces ramosus* peroxidase; BP1, barley peroxidase; CCP, cytochrome *c* peroxidase; CCP(MI), cytochrome *c* peroxidase expressed in *E. coli* containing Met-Ile at the N-terminus; CIP, *Coprinus cinereus* peroxidase expressed in *Aspergillus oryzae*; HRP-C, horseradish peroxidase isoenzyme *C*; SBP, soybean peroxidase; metMb, met-myoglobin; R48L, Arg48→Leu CCP(MI) mutant; R51L, Arg51→Leu CIP mutant; R38L, Arg38→Leu HRP-C mutant; W51F, Trp51→Phe CCP mutant; F54W, Phe54→Trp CIP mutant; D235N, Asp235→Asn CCP mutant; D245N, Asp245→Asn CIP mutant; H52L, His52→Leu CCP mutant; H41L, His41→Leu HRP-C mutant; wt, wild-type; IR, infrared; RR, resonance Raman; NMR, nuclear magnetic resonance; 5-c and 6-c, five-coordinate and six-coordinate hemes; HS, high-spin; CT1, long-wavelength (>600 nm) porphyrin-to-metal charge transfer band.

S0006-2960(97)00248-1 CCC: $14.00

ligand. This movement does not occur when NO and CO are bound at the iron, and so both ligands are beyond the maximal possible distance for hydrogen-bonding. Whether or not His52 hydrogen-bonds with CO and NO is less certain. This residue is close enough to the ligand, but the hydrogen bond geometry is poor and, moreover, the His must operate as a hydrogen bond acceptor (see above). In accord with these observations, previous RR and IR experiments on the CCP−CO complex in solution revealed that the oxygen atom of the bound CO is strongly hydrogen-bonded with a distal residue (Smulevich et al., 1988b), subsequently identified as the distal Arg (Smulevich et al., 1991b). Similar conclusions have also been reached on the HRP−CO complex by an IR examination of the pH dependence of the CO stretching vibration (Holzbaur et al., 1996). For this latter protein, on the basis of RR studies, the involvement of the distal residues in the stabilization of the CN^- (Al-Mustafa & Kincaid, 1994) and OH^- ligand (Feis et al., 1994; Howes et al., 1997) has also been proposed. In particular, for the HRP−OH complex, it appears that both the distal Arg and His participate, in a concerted manner, in hydrogen-bonding interactions with the ligand. The distal Arg is strongly hydrogen-bonded to the ligand (without a positive guanidinium group present, the hydroxyl is not able to bind to the iron atom), whereas the distal His plays a secondary role, but is also hydrogen-bonded to the bound ligand, giving rise to a 6-c LS heme (Howes et al., 1997). On the other hand, metMb binds the OH^- group, but no evidence has been found for the presence of hydrogen bonds which stabilize the ligand and, therefore, a 6-c HS complex is observed.

In the present work, we focus our interest on the RR and electronic absorption spectra of the fluoride adducts of different peroxidases belonging to the three classes of the plant peroxidase superfamily, together with some selected mutants in the distal cavity, and compared them with those of Mb. It is known that the three structural classes have less than 20% sequence identity, but they have conserved residues, namely, the distal His and Arg, and the proximal His hydrogen-bonded with an Asp residue (Welinder, 1992). On the distal side of the heme pocket, CCP (class I) contains the Trp51 residue, whereas the other two classes are characterized by the presence of a Phe residue in the corresponding position. Upon fluoride binding, all the peroxidases under investigation give rise to 6-coordinate high-spin complexes with the ν_{10} RR band of the porphyrin chromophore occurring near 1610 cm^{-1} (Choi et al., 1982) and, therefore, not interfering with the observation of the ν(C═C) stretching modes of the vinyl groups which occur in the 1620−1630 cm^{-1} region. Furthermore, the electronic absorption spectra are characterized by the presence of a charge transfer band (CT1) around 610−620 nm. It has recently been observed that the wavelength of this band depends on the p and π donor capability of the axial ligands (Smulevich et al., 1996b, 1997). It is expected, therefore, that its wavelength maximum varies in relation to the number and polarity of the hydrogen bonds involving the fluoride anion. The comparative analysis of the spectra of the various proteins has allowed us to differentiate the roles played by the different distal residues in stabilizing the sixth axial ligand. Moreover, this study has significant implications for the correlation between the vibrational and electronic features of the heme with the conjugated vinyl substituents.

MATERIALS AND METHODS

Recombinant *Coprinus cinereus* peroxidase (CIP) and CIP mutants were a gift from by Dr. K. G. Welinder (Copenhagen University) and were obtained by expression in transformed *A. oryzae* (Dalbøge et al., 1992). They were purified as previously described (Smulevich et al., 1994a, 1996b). Cytochrome *c* peroxidase and its site-directed mutants expressed in *Escherichia coli* CCP(MI) were obtained as described previously (Fishel et al., 1987; Smulevich et al., 1988a). Horseradish peroxidase (HRP-C, type VI-A) was purchased from Sigma (type VI-A, $R_z = 3.1$) and purified as described previously (Smulevich et al., 1991a). Horse heart myoglobin (metMb) was purchased from Sigma and used without further purification.

Peroxidase complexes with sodium fluoride (NaF Merck) were made by adding NaF (1 M) to the peroxidase solutions, to give a final concentration of 0.1 M NaF in 0.025 M citric acid−sodium citrate buffer at pH 5.0. Peroxidase concentrations were determined spectrophotometrically and were 0.1−0.4 mM for resonance Raman spectra and 10 times more diluted for UV−visible absorption spectra.

Absorption spectra were measured with a Cary 5 spectrophotometer. These spectra were measured both prior and after RR measurements to determine whether sample degradation had occurred. No degradation was detected under the experimental conditions applied in this study.

The resonance Raman (RR) spectra were obtained by excitation with the 406.7 and 413.1 nm lines of a Kr^+ laser (Coherent, Innova 90/K). The back-scattered light from a slowly rotating NMR tube was collected and focused into a computer-controlled double monochromator (Jobin-Yvon HG 2S), equipped with a cooled photomultiplier (RCA C31034 A) and photon counting electronics. The RR spectra were calibrated to an accuracy of 1 cm^{-1} for intense isolated bands, with indene as a standard.

Polarized spectra were obtained by inserting a polaroid analyzer between the sample and the entrance slit of the spectrometer. The depolarization ratios, ρ, of the bands at 314 and 460 cm^{-1} of CCl_4 were measured to check the reliability of the polarization measurements using a rotating NMR tube with 180° back-scattered geometry. The values obtained, 0.73 and 0.00, compare favorably with the theoretical values of 0.75 and 0.00, respectively.

RESULTS

Figure 1 shows the electronic absorption spectra of the fluoride adducts of met-myoglobin (Mb), horseradish peroxidase (HRP), *Coprinus cinereus* peroxidase (CIP), and recombinant cytochrome *c* peroxidase [CCP(MI)]. At pH 5.0, Mb, HRP, and CCP(MI) are fully bound with the fluoride, giving rise to a spectrum typical of a 6-coordinate high-spin heme (6-c HS) (Beetlestone & George, 1964; Asher et al., 1981; Tamura, 1971; Yonetani et al., 1966), whereas CIP shows the presence of a small amount of unligated protein, also seen in the NMR spectra (Veitch et al., 1996), as judged by the presence of a weak shoulder around 650 nm, previously assigned to the charge transfer band (CT1) of the 5-coordinate high-spin species (5-c HS) (Smulevich et al., 1994a, 1996b).

Some differences are observed in the wavelength of the absorption maxima. In particular, the wavelength of the CT1 band is at 617 nm for CCP(MI), 615 nm for CIP, and around 610 nm for both Mb and HRP. This latter protein is also

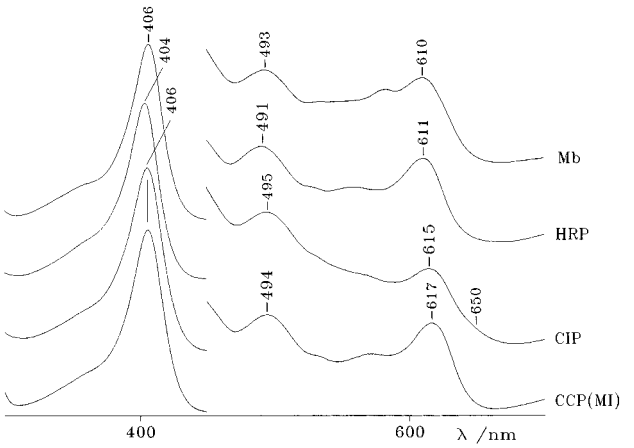

FIGURE 1: Electronic absorption spectra of the fluoride adducts of Mb, HRP, CIP, and CCP(MI) taken at pH 5.0. The region between 450 and 700 nm has been expanded 2.5 times.

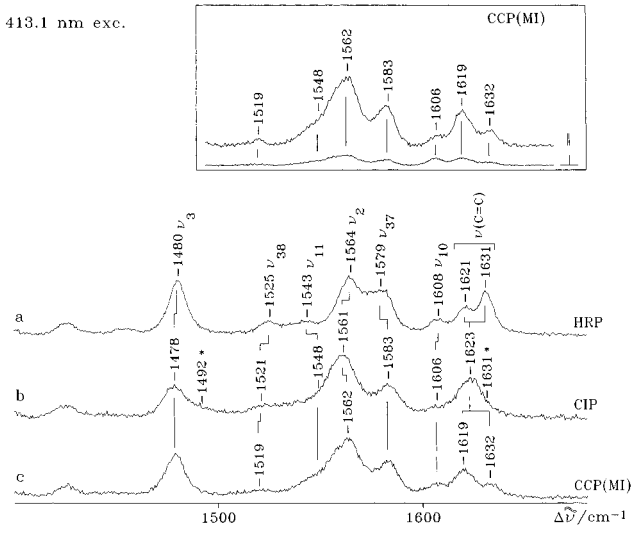

FIGURE 2: RR spectra of the fluoride adducts of HRP (a), CIP (b), and CCP(MI) (c) taken at pH 5.0. Experimental conditions: 413.1 nm excitation wavelength, 5 cm^{-1} resolution; (a) 3 s/0.5 cm^{-1} collection interval and 15 mW laser power at the sample; (b) 3 s/0.5 cm^{-1} collection interval and 10 mW laser power at the sample; (c) 2 s/0.5 cm^{-1} collection interval and 15 mW laser power at the sample. In the inset, the RR spectra of the CCP(MI)−F complex in perpendicular (⊥) and parallel (∥) polarized light are shown. Experimental conditions are as given above, except 48 s/0.5 cm^{-1} (⊥) and 13 s/0.5 cm^{-1} (∥) collection intervals were used.

characterized by a blue-shifted Soret band compared with the other heme proteins.

Figure 2 shows the corresponding resonance Raman (RR) spectra obtained for the three peroxidases. In the inset, the spectra in polarized light of the CCP(MI)−F complex are reported. The band assignments were obtained by analysis of all the spectra in polarized light (data not shown). The core size marker bands are characteristic of a 6-c HS heme which is in agreement with the electronic absorption spectra (Hashimoto et al., 1986; Palanappian & Terner, 1989) except that CIP shows weak bands due to the unligated form (indicated in the figure by an asterisk).

The frequency and intensity of the bands differ to some extent [for example, the core size marker bands ν_3, ν_2, and ν_{10} occur at slightly higher frequencies for HRP than CIP and CCP(MI)] and appear particularly changed in the region of the vinyl stretching modes. Two vinyl stretches are observed for both CCP(MI) and HRP at about 1620 and 1630 cm^{-1} with opposite relative intensity, whereas in CIP the

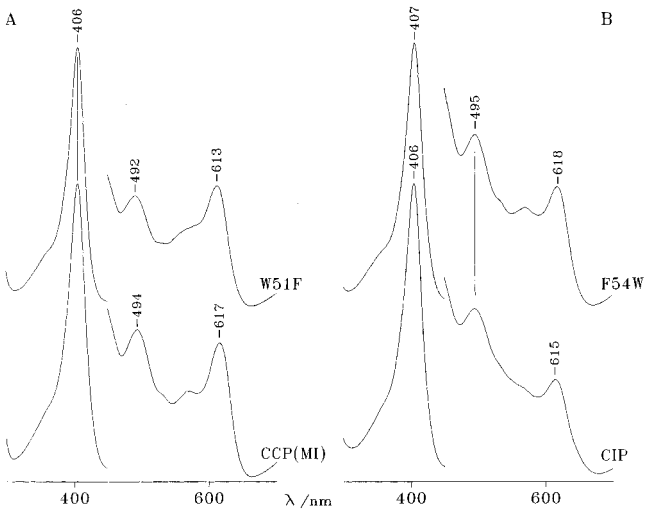

FIGURE 3: Electronic absorption spectra of the fluoride adducts of (A) CCP(MI) and its W51F mutant and (B) CIP and its F54W mutant taken at pH 5.0. The region between 450 and 700 nm has been expanded 3 times.

ν(C═C) stretching modes merge into a single band at 1623 cm^{-1}. The two vinyl stretches for the CCP−F complexes have not been assigned before, and in fact, the band at about 1620 cm^{-1} was wrongly assigned to the ν_{10} mode (Hashimoto et al., 1986). The band at about 1630 cm^{-1} has been previously observed only upon 514.5 nm excitation, but not assigned (Sievers et al., 1979).

To elucidate the roles played by the heme cavity residues in stabilizing the ligand, we undertook a detailed study of the F^- complexes of various site-directed mutants of the three peroxidases. The effect of mutation of the distal residues is shown in Figure 3. Panel A compares the electronic absorption spectra of the fluoride complexes of CCP(MI) with that of the Trp51→Phe (W51F) mutant, in which the distal tryptophan, that is hydrogen-bonded to a water molecule positioned above the Fe atom in the ferric structure (Finzel et al., 1984), is replaced by the non-hydrogen-bonding residue Phe (Wang et al., 1990). The mutation does not affect the ability of the Fe atom to bind fluoride, but the wavelengths of the bands in the visible region of its absorption spectrum are blue-shifted with respect to the spectrum of the parent enzyme. On the contrary, replacement of Phe54 with Trp (F54W) in CIP (position 54 in CIP corresponds to position 51 in CCP) causes a red-shift of the CT1 band by 3 nm with respect to the parent enzyme (panel B), giving rise to an absorption spectrum very similar to that obtained for wild-type CCP. In addition, no unligated species is detected in the fluoride adduct of the F54W mutant of CIP. The RR spectra of the fluoride complexes of the W51F CCP mutant and the F54W CIP mutant are very similar to the spectra of their corresponding parent enzyme (data not shown).

Fluoride affinity appears to be changed markedly upon mutation of the distal Arg or His in peroxidases. For CCP, the Arg→Leu and the His→Leu mutations decrease the affinity for fluoride by 900-fold (K_b = 26.3 mM) and 30-fold (K_b = 0.87 mM), respectively, as compared to wt CCP (K_b = 0.03 mM). The electronic absorption spectra of the corresponding mutants of HRP (R38L and H41L) and CIP (R51L) indicate that these mutations also cause significant decreases in the affinity for fluoride. In the presence of 0.1 M NaF, the absorption spectra for each of these mutants showed the enzyme to be predominantly in the unligated

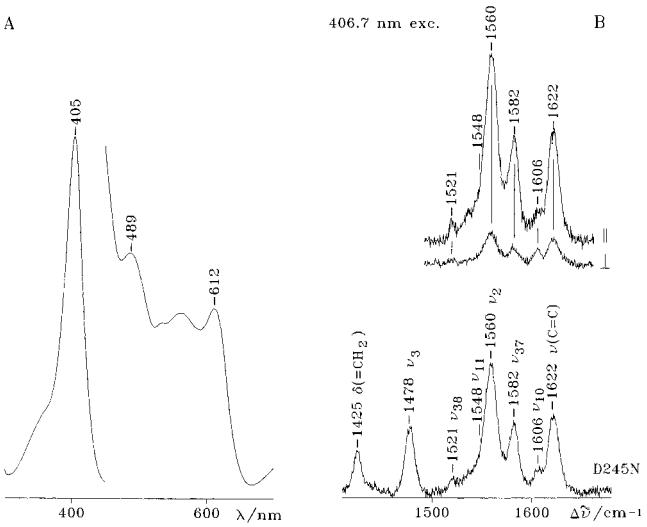

FIGURE 4: Fluoride adduct of D245N CIP mutant taken at pH 5.0. (A) Electronic absorption spectra; the region between 450 and 700 nm has been expanded 4 times. (B) RR spectra; experimental conditions: 406.7 nm excitation wavelength, 5 cm^{-1} resolution; (a) 5 s/0.5 cm^{-1} collection interval and 15 mW laser power at the sample. In the inset, the RR spectra in perpendicular (⊥) and parallel (∥) polarized light are shown. Experimental conditions are as given above, except 18 s/0.5 cm^{-1} (⊥) and 8 s/0.5 cm^{-1} (∥) collection intervals were used.

state, with a small amount of the fluoride complex present. The latter species in the H41L HRP mutant displayed the same features as the fluoride adducts of the parent enzymes (data not shown).

Figure 4 shows the electronic absorption spectrum (panel A) and the RR spectra (panel B) of the Asp245→Asn (D245N) mutant of CIP. The proximal aspartate carboxylate group of Asp 245 acts as hydrogen bond acceptor to the proximal His183 ligand of the heme Fe. When this residue is replaced by a carboxamide group, the protein fully binds the F^- (at 0.1 M NaF) as previously observed by NMR (Veitch et al., 1996). The electronic absorption spectrum slightly differs from that of the parent enzyme, being characterized by bands at 405, 489, and 612 nm. On the other hand, the core size marker bands in the RR spectrum maintain the same frequencies as CIP with two overlapped vinyl stretching modes at 1622 cm^{-1}, as indicated by the RR spectra taken in polarized light (panel B, upper spectra). Interestingly, the hyperfine-shifted resonances representing the heme group region in the NMR spectrum of F-bound−D245N CIP mutant are different from those of the wild-type F−CIP complex (Veitch et al., 1996).

Table 1 reports a summary of the absorption maxima wavelengths of the Soret and CT1 transitions together with the RR frequencies of the vinyl stretches for the fluoride complexes of various peroxidases, selected mutants, and myoglobin. The RR frequencies of the vinyl stretching modes observed for the corresponding unligated species are also reported for comparison. The last column indicates the proposed distal residues hydrogen-bonded to the fluoride ligand.

DISCUSSION

The heme iron ligand stabilization mechanism in heme proteins has been investigated through a number of structural, spectroscopic, thermodynamic, and kinetic studies of naturally occurring proteins and site-directed mutants. The conserved distal His in vertebrate myoglobins has been found to be a determining factor in controlling the ligand binding processes via hydrogen-bonding between the N_ϵ proton and the ligand. This mechanism has been recently confirmed by the X-ray structure of the fluoride adduct of ferric sperm whale Mb (Aime et al., 1996) where the fluoride anion, coordinated to the heme iron, was shown to be hydrogen-bonded to the distal His64 and to a water molecule (Wat195). Moreover, the H64V and H64L mutants of Mb, in which the distal His has been replaced by Val and Leu, respectively, lose the ability to bind fluoride (Ikeda-Saito et al., 1992). On the other hand, *Aplysia limacina* Mb, in which the distal His is replaced by Val, forms a fluoride complex. This apparent inconsistency with the corresponding Mb mutant has been clarified by the X-ray crystal structure of the fluoride derivative of *Aplysia limacina* Mb. The anion, coordinated to the heme iron, is hydrogen-bonded to Arg66, clearly indicating that in the absence of the distal His an alternative hydrogen bond donor has been selected to raise ligand affinity (Bolognesi et al., 1990).

The ligand stabilization mechanism in the plant peroxidase superfamily appears to be more complicated. These enzymes have conserved residues in the heme cavity, namely, the distal His and Arg, and the proximal His hydrogen-bonded

Table 1: Absorption Maxima (nm) of Soret and CT1 Bands, and RR Frequencies (cm^{-1}) of the ν(C=C) Vinyl Stretching Modes Observed for Fluoride Adducts of Various Heme Proteins Together with the ν(C=C) Vinyl Stretching Modes Observed for the Corresponding Unligated Species at pH 7.0 (Proposed Distal Hydrogen Bonds Involving the Ligand Are Also Given)

			ν(C=C)[a]		
protein	Soret	CT1	F^- complex, pH 5.0	ferric form, pH 7.0	H-bonds with F^-
CCP(MI)	406	617	1619, 1632	1618[b]	H_2O, R48, W51[c]
H52L CCP	406	617			H_2O, R48, W51[c]
W51F CCP	406	613	1619, 1632	1617[b]	H_2O, R48
R48L CCP	406	610			W51
F54W CIP	407	618	1623	1624[d]	H_2O, R51, W54
CIP	406	~615	1623	1625[e]	H_2O, R51
D245N CIP	405	612	1622	1622[f]	R51
HRP	404	611	1621, 1631	1624, 1630[g]	H_2O, R38
BP1[h]	402	611	1630	1623, 1631	H_2O, R45
SBP[i]	402	610	1622, 1632	1622, 1632	H_2O, R38[j]
Mb	406	610	1622[k]	1621[l]	H_2O, H64[m]

[a] The most intense band is underlined. [b] Smulevich et al. (1988a, 1996a). [c] Edwards & Poulos, (1990). [d] F. Neri, B. Baldi, K. G. Welinder, and G. Smulevich, unpublished results. [e] Smulevich et al. (1994a). [f] Smulevich et al. (1996b). [g] Smulevich et al. (1994b). [h] D. B. Howes, C. B. Rasmussen, K. G. Welinder, and G. Smulevich, unpublished results. [i] M. Nissum, P. W. Jensen, and G. Smulevich, unpublished results. [j] From sequence data by K. G. Welinder, unpublished results. [k] Choi et al. (1982). [l] Hu & Spiro (1996). [m] Aime et al. (1996).

with a buried Asp side chain. In addition, the crystal structures of CCP (Finzel et al., 1984), pea cytosolic ascorbate peroxidase (Patterson & Poulos, 1995), lignin peroxidase (Piontek et al., 1993; Poulos et al., 1993), manganese peroxidase (Sundaramoorthy et al., 1994), *Arthromyces ramosus* peroxidase (ARP) (Kunishima et al., 1994, 1996), CIP (Petersen et al., 1994), and peanut peroxidase (Schuller et al., 1996) show that an extended hydrogen bond network connects the proximal and distal sides of the heme cavity through water molecules and the propionate groups of the heme. The similarity in the active site structure of peroxidases suggests a common mechanism for compound I formation during peroxidase catalysis, where ligand stabilization by the distal Arg is coupled to protonation of the distal His (Poulos & Fenna, 1994). The fact that mutants of peroxidases where the distal Arg is replaced by Leu have much weaker fluoride binding implies that ligand stabilization by the distal Arg plays an important role, mimicking that carried out in the catalytic mechanism. The crystal structure of the CCP−F complex shows that the Arg48 side chain moves about 2.5 Å toward the ligand to form a hydrogen bond with the bound fluoride (Edwards & Poulos, 1990). Thus, Arg48 stabilizes the fluoride complex by formation of charge-mediated hydrogen bonds with the bound F^-. This is seen by the blue-shift in the CT1 band upon mutation of Arg48 to Leu in CCP (see below). A similar movement of Arg48 accompanies compound I formation (Fülöp et al., 1994), and this interaction presumably stabilizes binding of the oxene dianion to the ferryl iron (Vitello et al., 1993). The distal His does not appear to stabilize the fluoride complex by hydrogen-bonding interactions. This is seen by the failure of the His52 to Leu mutation to change the position of the CT1 band (Table 1; see below). The result is consistent with the crystal structure of the CCP−F complex, which shows that although the His52 is less than 2.8 Å distant from the bound fluoride, its hydrogen-bonding geometry with F^- is poor (Edwards & Poulos, 1990) and the interaction between His52 and bound F^- appears to be via mutual hydrogen bonds with an active site water molecule. The stabilizing effect of the distal His on the F^- complex may instead result from its role as a proton acceptor. The equilibrium constant for F^-, CN^-, and HOOH binding in CCP, as well as other heme peroxidases, increases upon lowering the pH (Erman, 1974; DeLauder et al., 1994), which indicates that each of these anions binds to CCP as their conjugate acids. Previous work has shown that the distal His is the proton acceptor for binding of the peroxide anion (Erman et al., 1993), and it seems likely that it serves this function in fluoride binding as well. Loss of this acceptor would decrease the affinity for F^- by decreasing the bimolecular rate of HF binding. It is interesting to note that the peroxidases have a conserved structural feature that seems to promote the role of the distal His as a proton acceptor. In CCP, N_δ of the distal His is hydrogen-bonded to the side chain of Asn82, which will leave the N_ϵ atom free to accept a proton. This interaction, which should control the proton-acceptor and -donor properties of the distal His (Edwards & Poulos, 1990), is also evident in the lignin peroxidase structure (Edwards et al., 1992) and is predicted to be conserved in all the other peroxidases (Welinder et al., 1992).

Since the structure of no other peroxidase−fluoride complex has been solved, it was necessary to compare the spectroscopic results obtained for the CCP−F adduct with those obtained for the adducts of other peroxidases and some of their selected mutants in order to identify the residues involved in ligand stabilization. This important part of the investigation has been undertaken in the context of an analysis of the correlation between the wavelength of the electronic absorption bands (Soret, Q, and CT bands) and the effect of the different degree of conjugation of the two (C═C) bonds of the vinyl substituents, and also the correlation between the wavelength of the CT1 bands and the hydrogen-bonding interaction between the fluoride ligand and the distal residues.

$\pi\rightarrow\pi^*$ Transition Energy. The absorption maxima of the ferri-protoporphyrin IX prosthetic group are related to the coordination/spin state of the heme and to the degree of conjugation between the heme group and its two vinyl substituents, which together can cause up to 10 nm red-shift of the electronic transitions. Therefore, the electronic coupling between the vinyl groups and the porphyrin modulates the energy of the $\pi\rightarrow\pi^*$ transitions and furnishes an enhancement mechanism for the vibrational modes of the vinyls in the RR spectra (Spiro & Li, 1988). In most cases, the vinyl substituents give rise to polarized bands around 1620−1630 cm^{-1}. A lower frequency is expected to correspond to a higher degree of conjugation between the vinyl group and the porphyrin π system. Increased conjugation from the vinyl groups should shift the energy of the $\pi\rightarrow\pi^*$ transitions to lower energy, thus shifting the Soret maximum to the red. From the RR spectra and Table 1, it can be seen that the heme proteins examined here fall into two groups. CIP, its F54W and D245N mutants, and Mb show only one ν(C═C) mode around 1620 cm^{-1}; the F^- complexes of these proteins have a Soret maximum near 406 nm. On the other hand, HRP (Smulevich et al., 1994b), barley peroxidase (BP1) (D. B. Howes, C. B. Rasmussen, K. G. Welinder, and G. Smulevich, unpublished results), and soybean peroxidase (SBP) (M. Nissum, P. W. Jensen, and G. Smulevich, unpublished results) have two ν(C═C) modes around 1620 and 1630 cm^{-1}, the latter being more intense. The weaker conjugation of the vinyl side chains of these proteins is associated with a 2−4 nm blue shift of the Soret maximum relative to CIP and Mb (Table 1). CCP−F is an intermediate case, two stretching modes being observed, but the lowest frequency band is the most intense. Based on the position of the Soret maximum, this protein seems to be comparable to CIP and Mb.

It is interesting to note that the CCP−F adduct is the only example where the vinyl stretching mode frequencies vary with respect to the corresponding unligated form, showing a single band at 1618 cm^{-1} (Smulevich et al., 1988a, 1996a; Table 1). On the other hand, a similar frequency splitting (but with reverse intensity) has been observed for ferric CCP and its mutants at alkaline pH as a consequence of a protein conformational change (which allows the distal His52 to bind the Fe atom) in the acid/alkaline transition which specifically perturbs the 2-vinyl group (Smulevich et al., 1991b, 1996a). A conformational change can also be invoked in the case of the fluoride adduct of CCP, considering that the distal Arg48 moves in about 2.5 Å toward the fluoride anion.

Thus, proteins whose F^- complexes are characterized by an intense single vinyl stretch around 1620 cm^{-1} give rise to Soret maxima between 405 and 407 nm, and a CT1 band between 612 and 618 nm. Conjugation of the vinyl groups with the heme appears to be comparable for these proteins, and the absorption maxima of the proteins should therefore

be comparable. Accordingly, Mb−F, characterized by a single intense vinyl stretch at 1622 cm^{-1} (Choi et al., 1982), has a Soret maximum at 406 nm, like CCP and CIP. On the other hand, the CT1 band of Mb−F occurs at a very short wavelength (610 nm, Table 1) which indicates that its transition energy is influenced by an effect other than conjugation (see below). The plant peroxidases HRP, BP1, and SBP, whose RR spectra show one weak vinyl stretch around 1620 cm^{-1} and a second, very strong, stretch around 1630 cm^{-1}, give rise to an overall blue-shift in the electronic absorption spectra, indicating a lower degree of vinyl conjugation with respect to peroxidases belonging to classes I and II. Accordingly, both the Soret maximum and the CT1 maximum of these proteins are blue-shifted 2−4 nm with respect to CIP, which has a comparable number of distal hydrogen bond donors to the F^- ligand (see below).

Charge-Transfer Transition Energy. The band observed at 617 nm in CCP is due to the charge transfer transition from the porphyrin to the iron [$a'_{2u}(\pi) \rightarrow e_g(d_\pi)$]. It has been shown recently that the maximum of the CT1 band blue-shifts when the p and/or π donor capability of the axial ligands increases (Smulevich et al., 1995, 1996b, 1997; Howes et al., 1997). In fact, the interaction between the p orbitals of the ligand and the iron d_π orbitals raises the energy of the latter. In particular, hydrogen bonding affects the p donor capability. If the ligand acts as a hydrogen bond donor, then the stronger the hydrogen bond and the charge donation to the iron atom, the lower is the wavelength of the CT1 band. The opposite effect is observed when the ligand acts as hydrogen bond acceptor (Smulevich et al., 1996b). This trend is illustrated by the effect of distal mutations on CT1 of CCP−F. Among the native proteins, the longest wavelength for CT1 is observed for the fluoride complex of CCP, where the bound F^- receives hydrogen bonds from Arg48, Trp51, and a water molecule. A blue-shift of CT1 is observed in the mutant W51F where replacement of the distal Trp by a non-hydrogen-bonding Phe residue reduces the number of hydrogen bonds involving the ligand with the protein matrix from three to two. The loss of hydrogen bond donor Trp51 shifts the charge-transfer band to a position similar to that seen for native CIP, which also has only two H-bond donors capable of interacting with the F^- ligand. An even greater blue-shift is observed when the distal Arg is replaced with Leu. With the loss of Arg48 as hydrogen bond donor, the position of the charge-transfer band shifts to a position comparable to that seen for Mb−F. The other charge-transfer band (CT2) in the visible region (Vitello et al., 1993) is expected to follow the same behavior as the CT1 band. The overlap of CT2 with the β band precludes an accurate evaluation of its wavelength, however, and this band will not be considered further.

The distal Trp is conserved only in class I peroxidases (which includes CCP), while in classes II and III it is substituted by a Phe residue (Welinder & Gajhede, 1993). The W51F mutant of CCP should therefore represent a good model to mimic the fluoride complexes of the other two peroxidases under investigation. CIP (class II) has a lower affinity for fluoride than CCP, and, indeed, the absorption spectrum of the complex shows the presence of some nonligated form, as is also confirmed by the RR and NMR (Veitch et al., 1996) spectra. This makes it difficult to estimate the exact position of the CT bands, but the CT1 band appears to be blue-shifted compared to CCP. Replacement of the distal Phe54 with Trp not only increases the fluoride affinity, but also causes a red-shift of the CT1 band whose maximum becomes very similar to that of wild-type CCP, indicating that the mutated residue is hydrogen-bonded to the ligand.

Considering the previously discussed effect of reduced vinyl conjugation leading to a 4 nm blue-shift of the electronic absorption maxima of the fluoride adducts of HRP, BP1, and SBP, the CT1 wavelength of these proteins can be considered to be approximately equivalent to that of CIP. Therefore, we conclude that in CCP the fluoride ligand is stabilized by three hydrogen bonds, while for the other peroxidases under study, it is stabilized by two hydrogen bonds. In the absence of the distal Trp residue, one is with the distal Arg, and the other should be with a water molecule which is in turn hydrogen-bonded with the distal His. The X-ray structure of the Mb−F adduct shows that the anion is hydrogen-bonded with a water molecule and the distal His (Aime et al., 1996) and the observed CT1 band occurs at 610 nm, blue-shifted with respect to class II and III peroxidases. It is suggested that this difference might be ascribed to the different type of hydrogen bond involving the fluoride anion, i.e., with neutral His in myoglobin and with the positively charged guanidinium group of Arg in the peroxidases. This conclusion is reinforced by the observation that the CT1 maximum is comparable for Mb−F and the R48L mutant of CCP.

CIP shows a lower affinity for the fluoride ligand than the peroxidases of class III and CCP. The X-ray structure has not yet been solved for the class III peroxidases under study, but comparing the X-ray diffraction results obtained for the resting state of CCP (Finzel et al., 1984) and ARP/CIP (Kunishima et al., 1994, 1996; Petersen, 1995), it appears that the guanidinium group of the distal Arg is about 0.5 Å further away from the heme iron in ARP/CIP than in CCP. This could be responsible for a weaker interaction upon fluoride binding. On the contrary, the Asp245→Asn mutant of CIP appears to bind fluoride with much higher affinity, as previously observed by NMR (Veitch et al., 1996). Notwithstanding the fact that the higher affinity of the mutant with respect to the parent enzyme can simply derive from the movement of the iron toward the heme plane, as a consequence of the rupture or weakening of the proximal hydrogen bond between His183 and Asp245, a concomitant approach of the Arg to the distal ligand can also be invoked. This second driving mechanism is suggested on the basis of the recent study of the ferric form of this mutant at alkaline pH where a novel feature was observed and assigned to a 5-coordinate high-spin species with a hydroxyl group bound to the iron atom and strongly hydrogen-bonded to the distal Arg51 (Smulevich et al., 1996b). The corresponding D235N CCP mutant shows an absorption spectrum identical to that of wild-type CCP (data not shown) with a CT1 band at 617 nm. Therefore, the 5 nm blue-shift of the CT1 band of the corresponding D245N CIP mutant suggests that in this latter case only the Arg residue is hydrogen-bonded to the fluoride anion.

In conclusion, the present work highlights the different mechanisms of stabilization of the fluoride ligand exerted by the distal residues in Mb and peroxidases. For these latter proteins, the Arg is determinant in controlling the ligand binding via a strong hydrogen bond between the positively charged guanidinium group and the anion. The distal His plays a minor, but important, role by accepting a proton from HF and hydrogen-bonding probably through a water mol-

ecule with the anion (as in CCP). For Mb, the distal His is solely responsible for stabilization of the exogenous ligands; when this residue was mutated by Val or Leu, the proteins lost the ability to bind fluoride ion (Ikeda-Saito et al., 1992). The only exception, to our knowledge, occurs for *Aplysia limacina* Mb, where the absence of the distal His is partially compensated for by the presence of an arginine residue at position 66. This residue, upon ligand binding, folds into the distal site and interacts via a hydrogen bond with the anion (Bolognesi et al., 1990; Aime et al., 1996).

The present work confirms that the wavelength of the CT1 band is a sensitive probe of axial ligand polarity and of its interaction with the distal protein residues. In addition, combined analysis of the vibrational and electronic spectra allows one to rationalize the wavelength of the $\pi \rightarrow \pi^*$ transition in terms of the degree of conjugation between the porphyrin macrocycle and the vinyl substituents.

ACKNOWLEDGMENT

We thank Prof. M. P. Marzocchi (Universita' di Firenze) and Dr. K. G. Welinder (Copenhagen University) for very helpful discussions.

REFERENCES

Aime, S., Fasano, M., Paoletti, S., Cutruzzola, F., Desideri, A., Bolognesi, M., Rizzi, M., & Ascenzi, P. (1996) *Biophys. J. 70*, 482.

Allentoff, A. J., Bolton, J. L., Wilks, A., Thompson, J. A., & Ortiz de Montellano, P. R. (1992) *J. Am. Chem. Soc. 114*, 9744.

Al-Mustafa, J., & Kincaid, J. (1994) *Biochemistry 33*, 2191.

Antonini, E., & Brunori, M. (1971) in *Hemoglobin and myoglobin in their reaction with ligands*, pp 1−12, 40−54, 219−285, Elsevier North-Holland Publishing Co., Amsterdam and London.

Asher, S. A., Adams, M. L., & Schuster, T. M. (1981) *Biochemistry 20*, 3339.

Beetlestone, J., & George, P. (1964) *Biochemistry 3*, 707.

Bolognesi, M., Coda, A., Frigerio, F., & Gatti, G. (1990) *J. Mol. Biol. 213*, 621.

Choi, S., Spiro, T. G., Langry, K. G., Smith, K. M., Budd, D. L., & LaMar, G. N. (1982) *J. Am. Chem. Soc. 104*, 4345.

Dalbøge, H., Jensen, E. B., & Welinder, K. G. (1992) Patent application No. WO 92/16634.

Dawson, J. H. (1988) *Science 240*, 433.

DeLauder, S. F., Mauro, J. M., Poulos, T. L., Williams, J. C., & Schwarz, F. P. (1994) *Biochem. J. 302*, 437.

Edwards, S. L., & Poulos, T. L. (1990) *J. Biol. Chem. 265*, 2588.

Edwards, S. L., Raag, R., Wariishi, H., Gold, M. H., & Poulos, T. L. (1992) *Proc. Natl. Acad. Sci. U.S.A. 90*, 750.

Erman, J. E. (1974) *Biochemistry 13*, 34.

Erman, J. E., Vitello, L. B., Miller, M. A., Shaw, A., Brown, K. A., & Kraut, J. (1993) *Biochemistry 32*, 9798.

Feis, A., Paoli, M., Marzocchi, M. P., & Smulevich, G. (1994) *Biochemistry 33*, 4577.

Finzel, B. C., Poulos, T. L., & Kraut, J. (1984) *J. Biol. Chem. 259*, 13027.

Fishel, L. A., Villafranca, J. E., Mauro, J. M., & Kraut, J. (1987) *Biochemistry 26*, 351.

Fülöp, V., Phizackerley, R. P., Soltis, S. M., Clifton, I. J., Wakatsuki, S., Erman, J., & Edwards, S. L. (1994) *Structure 2*, 24.

Hashimoto, S., Teraoka, J., Inubishi, T., Yonetani, T., & Kitagawa, T. (1986) *J. Biol. Chem. 261*, 11110.

Holzbaur, I. E., English, A. M., & Ismail, A. A. (1996) *J. Am. Chem. Soc. 118*, 3354.

Howes, B. D., Rodriguez-Lopez, N. J., Smith, A. T., & Smulevich, G. (1997) *Biochemistry 36*, 1532.

Hu, S., Smith, K. M., & Spiro, T. G. (1996) *J. Am. Chem. Soc. 118*, 12638.

Ikeda-Saito, M., Hori, H., Andersson, L. A., Prince, R. C., Pickering, I. J., George, G. N., Sanders, C. R., II, Lutz, R. S., McKelvey, E. J., & Mattera, R. (1992) *J. Biol. Chem. 267*, 22843.

Kunishima, N., Fukuyama, K., Matsubara, H., Hatanaka, H., Shibano, Y., & Amachi (1994) *J. Mol. Biol. 235*, 331.

Kunishima, N., Amada, F., Fukuyama, K., Kawamoto, M., Matsunaga, T., & Matsubara, H. (1996) *FEBS Lett. 378*, 291.

Miller, M. A., Shaw, A., & Kraut, J. (1994) *Nat. Struct. Biol. 1*, 524.

Palanappian, V., & Terner, J. (1989) *J. Biol. Chem. 264*, 16046.

Patterson, W. R., & Poulos, T. L. (1995) *Biochemistry 34*, 4331.

Petersen, J. F. W. (1995) Ph.D. Thesis, University of Copenhagen, Denmark.

Petersen, J. F. W., Kodziola, A., & Larsen, S. (1994) *FEBS Lett. 399*, 291.

Piontek, K., Glumoff, T., & Winterhalter, K. (1993) *FEBS Lett. 315*, 119.

Poulos, T. L., & Kraut, J. (1980) *J. Biol. Chem. 255*, 8199.

Poulos, T. L., & Fenna, R. E. (1994) in *Metal Ions in Biological Systems* (Siegel, H., Ed.) pp 25−75, Marcel Dekker, New York.

Poulos, T. L., Edwards, S. L., Wariishi, H., & Gold, M. H. (1993) *J. Mol. Biol. 268*, 4429.

Schuller, D. J., Ban, N., van Huytee, R. B., McPherson, A., & Poulos, T. L. (1996) *Structure 4*, 311.

Sievers, G., Österlund, K., & Ellfolk, N. (1979) *Biochim. Biophys. Acta 581*, 1.

Sitter, A. J., Reczeck, C. M., & Terner, J. (1985) *J. Biol. Chem. 260*, 7515.

Smulevich, G., Mauro, J. M., Fishel, L. A., English, A. M., Kraut, J., & Spiro, T. G. (1988a) *Biochemistry 27*, 5477.

Smulevich, G., Mauro, J. M., Fishel, L. A., English, A. M., Kraut, J., & Spiro, T. G. (1988b) *Biochemistry 27*, 5486.

Smulevich, G., English, A. M., Mantini, A. R., & Marzocchi, M. P. (1991a) *Biochemistry 30*, 772.

Smulevich, G., Miller, M. A., Kraut, J., & Spiro, T. G. (1991b) *Biochemistry 30*, 9546.

Smulevich, G., Feis, A., Focardi, C., Tams, J., & Welinder, K. G. (1994a) *Biochemistry 33*, 15425.

Smulevich, G., Paoli, M., Burke, J. F., Sanders, S. A., Thorneley, R. N. F., & Smith, A. T. (1994b) *Biochemistry 33*, 7398.

Smulevich, G., Neri, F., Willemsen, O., Choudhury, K., Marzocchi, M. P., & Poulos, T. L. (1995) *Biochemistry 34*, 13485.

Smulevich, G., Hu, S., Rodgers, K. R., Goodin, D. B., Smith, K. M., & Spiro, T. G. (1996a) *Biospectroscopy 2*, 365.

Smulevich, G., Neri, F., Marzocchi, M. P., & Welinder, K. G. (1996b) *Biochemistry 35*, 10576.

Smulevich, G., Paoli, M., De Sanctis, G., Mantini, A. R., Ascoli, F., & Coletta, M. (1997) *Biochemistry 36*, 640.

Spiro, T. G., & Li, X.-Y. (1988) in *Biological Application of Raman Spectroscopy* (Spiro, T. G., Ed.) Vol. 3, pp 1−37, Wiley Interscience, New York.

Sundaramoorthy, M., Kishi, K., Gold, M. H., & Poulos, T. L. (1994) *J. Mol. Biol. 238*, 845.

Tamura, M. (1971) *Biochim. Biophys. Acta 243*, 249.

Veitch, N. C., Gao, Y., & Welinder, K. G. (1996) *Biochemistry 35*, 14370.

Vitello, L. D., Erman, J. E., Miller, M. A., Wang, J., & Kraut, J. (1993) *Biochemistry 32*, 9807.

Wang, J., Mauro, J. M., Edwards, S. L., Oatley, S. J., Fishel, L. A., Ashford, V. A., Xuong, N., & Kraut, J. (1990) *Biochemistry 29*, 7160.

Welinder, K. G. (1992) *Curr. Opin. Struct. Biol. 2*, 388.

Welinder, K. G., & Gajhede, M. (1993) in *Plant peroxidases: Biochemistry and Physiology* (Welinder, K. G., Rasmussen, S. K., Penel, C., & Greppin, H., Eds.) pp 35−42, University of Geneva, Switzerland.

Welinder, K. G., Mauro, M., & Norskov-Lauritsen, L. (1992) *Biochem. Soc. Trans. 20*, 337.

Yonetani, T., & Schleyer, H. L. (1967) *J. Biol. Chem. 242*, 1974.

Yonetani, T., Wilson, B. F., & Seamonds, B. (1966) *J. Biol. Chem. 241*, 5347.

BI970248+